Normal and Surface-Enhanced Raman Spectroscopy of Nitroazobenzene Submonolayers and Multilayers on Carbon and Silver Surfaces

HAIHE LIANG, HONG TIAN, and RICHARD L. McCREERY*

Department of Chemistry, The Ohio State University, 100 W 18th Avenue, Columbus, Ohio 43210 (H.L., H.R.); and Department of Chemistry, National Institute for Nanotechnology, University of Alberta, Canada, T6G 2G2 (R.L.M.)

Raman and ultraviolet–visible (UV-Vis) absorption spectra were obtained for nitroazobenzene (NAB) chemisorbed on smooth and rough silver, and they were compared to published spectra for NAB on sp^2 hybridized pyrolyzed photoresist film (PPF) surfaces. High signal-to-noise ratio Raman spectra were obtained for 4.5 nm thick NAB films on PPF and smooth Ag due to significant enhancement of the NAB scattering relative to that observed in solution. The UV-Vis spectra of chemisorbed NAB exhibited a significant shift toward longer wavelength, thus bringing the NAB absorption closer to the 514.5 nm laser wavelength. The red shift was larger for PPF than for smooth Ag, consistent with the ~5× stronger Raman signal obtained on PPF. Deposition of Ag onto quartz without a chromium adhesion layer produced a rough Ag surface that enhanced the Raman spectrum of chemisorbed NAB by a factor of ~1000, as expected for roughened Ag due to electromagnetic field enhancement. The strong Raman signal permitted observation of NAB at low coverage and revealed changes in the NAB spectrum as the film progressed from submonolayer to multilayer thicknesses. Finally, deposition of Ag onto PPF/NAB samples through a metal grid produced Ag squares on top of the NAB, which enhanced the Raman scattering of the NAB layer by a factor of ~100. Deposition of a final conducting film on the Ag squares should permit *in situ* observation of a wide range of molecules in operating molecular electronic junctions.

Index Headings: **Raman; Surface-enhanced Raman scattering; SERS; Surface; Molecular electronics; Chemisorption.**

INTRODUCTION

Molecular electronics has been a very active area of research for approximately the last decade, with one primary objective being to relate molecular structure to electronic behavior.[1–8] Many paradigms for studying the electronic properties of molecules involve single molecule experiments, primarily with scanning probe techniques and in some cases inelastic tunneling spectroscopy.[8–10] Elegant experiments measuring single molecule conductance have been reported, as have observations of molecular orbitals of single molecules.[11–14] However, sensitivity limitations generally prevent the application of optical spectroscopy to single molecule electronic junctions, with the result being a significant constraint on determination of junction structure.[15] Molecular junctions consisting of a large number of molecules (10^6–10^{12}) in parallel have been probed with Raman and infrared spectroscopy because the junction size is compatible with the optical beam dimensions.[7,16,17] In the case of Raman spectroscopy, structural changes inside a molecular junction under bias were observed and were related to the electronic conductance of the junction.[16,17] In that case, the nitroazobenzene (NAB) molecule

studied was chosen for its strong resonance Raman activity, thus providing the sensitivity required to monitor molecular layers in the range of 1.5 to 5 nm thick. While Raman spectra are valuable for deducing structural changes in molecular junctions, the requirement of resonance enhancement significantly decreases the generality of the method.

In addition to *in situ* monitoring of NAB/TiO$_2$ molecular junctions, Raman spectroscopy revealed an unexpected enhancement mechanism when the NAB was bonded to an sp^2 hybridized carbon surface.[18,19] The Raman cross-section for NAB covalently bonded to a carbon surface was 100 to 1000 times higher than that of NAB in CCl$_4$ solution, and the surface spectrum was qualitatively different from the solution or solid spectra of NAB. In an initially unrelated study, we reported that molecular junctions could be fabricated with silver as one of the "contacts" instead of gold or copper.[20] Given the well-known activity of Ag for surface-enhanced Raman spectroscopy (SERS), there may be advantages to exploiting SERS for monitoring junction structure and dynamics. Accordingly, the current investigation was undertaken with several objectives in mind. First, we sought to obtain Raman spectra of NAB films with low coverage in order to observe structural evolution of the NAB film from monolayer to multilayer thicknesses. Second, we examined conditions for obtaining SERS spectra in complete molecular junctions by inserting Ag islands on top of the molecular layer before deposition of a Au top contact. Third, we investigated the unusual enhancement observed for NAB on carbon surfaces by comparison to a Ag substrate. The approach involves both Raman and ultraviolet–visible (UV-Vis) spectroscopy of NAB on smooth Ag, rough Ag islands, and pyrolyzed photoresist films (PPF).

EXPERIMENTAL

The PPF films were prepared as described previously[21,22] for the case of approximately 2 μm thick films on SiO$_2$/Si. Optically transparent PPF was prepared as described by Donner et al.[23] by diluting the photoresist reagent by a factor of 20 (v/v) with 1-methoxy-2-propanol acetate. The diluted solution of photoresist was spin coated onto a 2 × 4 cm quartz slide, then pyrolyzed to yield a PPF film that appeared gray in color on the quartz slide. The quartz/PPF sample was 50–80% transparent for the 200 to 800 nm wavelength range, with an absorption maximum at 270 ± 4 nm. Based on reported optical constants for glassy carbon,[24] commercial software (Filmstar) was used to estimate the PPF thickness from its optical transmission to be 9 ± 1 nm. NAB was bonded to the transparent PPF by electrochemical reduction of NAB diazonium ion after sputtering an approximately 100 Å thick

gold rectangle around the edges of the sample to reduce ohmic losses in the PPF. The PPF area not covered by gold was 0.4 × 1.5 cm, with the longer axis parallel to the slit image of the UV-Vis spectrometer.

The nitroazobenzene diazonium reagent was prepared as the tetrafluoroborate salt, as reported previously, and stored in a freezer.[21] NAB diazonium salt solutions were prepared fresh daily in acetonitrile. Ag films were prepared by electron beam deposition onto silicon surfaces on which 200 nm of SiO_2 had been grown by wet oxidation. The Si/SiO_2 samples were sonicated for 1 minute each in acetone, Nanopure water (Barnstead, 18 MΩ), and isopropyl alcohol. To prepare smooth Ag films, 4 nm Cr was deposited at a rate of 0.1 nm/s followed by 20 nm of silver at a rate of 0.1 nm/s onto the Si/SiO_2 samples, with a backpressure of $\sim 2 \times 10^{-6}$ torr. To make rough Ag surfaces, 10 nm of Ag was deposited directly on Si/SiO_2 at a rate of 0.1 nm/s, without the Cr adhesion layer. For experiments involving UV-Vis transmission through the metal/molecule films, quartz was substituted for Si/SiO_2.

The atomic force microscopy (AFM) image of the smooth Ag surface was featureless except for occasional large particles, while the image of the rough surface was dominated by circular features with diameters in the range of <0.1 μm to ~0.3 μm. The root mean square (rms) roughness of a 10 μm × 10 μm AFM image of the smooth Ag surface was 1.1 nm, while a line profile of the smooth surface had an rms roughness of 0.9 nm. For the rough Ag surface, the rms for a 10 μm × 10 μm area was 6.8 nm, while that of a line profile was 5.8 nm. The maximum height of the features on rough Ag observed with AFM was approximately 35 nm, implying that they have the shape of islands rather than spheres. Several authors have described the SERS activity of Ag islands prepared in a similar fashion, with often very large EM field enhancements reported.[25–29]

The NAB was bonded to Ag spontaneously by exposing the Ag to a 1 mM solution of NAB diazonium tetrafluoroborate in acetonitrile for 2 minutes, unless noted otherwise. The SiO_2/Ag samples were first rinsed for 1 minute each in acetone, nanopure water, and isopropanol, then immediately dipped in the NAB diazonium solution. A final rinse with acetonitrile removed excess diazonium reagent. As noted below, lower concentrations of diazonium reagent and shorter deposition times were employed to reduce the NAB coverage on Ag. The thicknesses of NAB films on smooth Ag were determined with AFM "scratching"[30] as well as ellipsometry. In the latter technique, the refractive index of NAB was assumed to equal 1.75, with a negligible absorption coefficient (i.e., $k = 0$). Two AFM "scratches" with areas of 2 μm × 2 μm on a sample of NAB on smooth Ag (2 minute exposure, 1 mM NAB diazonium ion) were analyzed to yield a NAB thickness of 4.6 ± 0.2 nm. Ten smooth Ag samples treated the same way and examined by ellipsometry yielded an average thickness of 4.4 nm with a standard deviation of 0.4 nm. An isolated NAB molecule is 1.35 nm long, so an approximately 4.5 nm thick multilayer implies a layer thickness of at least three NAB molecules.

Raman spectra of NAB were also obtained on PPF, both before and after deposition of Ag squares with dimensions of approximately 50 × 50 μm. PPF was prepared by pyrolysis of positive photoresist as described previously,[21,22,31] followed by electrochemical deposition of a 4.5 nm film of NAB. Then 10 nm of Ag was deposited at $\sim 2 \times 10^{-6}$ torr on the NAB/PPF through a 300 lines/inch Ni grid, purchased from Buckbee Mears, resulting in a regular array of Ag squares on top of the NAB.

Raman spectra were obtained with a 514.5 nm laser and a custom line-focused $f/2$ spectrograph (Chromex)[32] with an Andor back-thinned charge-coupled device (CCD) detector cooled to −85 °C. As described previously, the line-focused configuration significantly reduced the laser power density at the sample and reduced radiation damage.[32] Using a point-focused spectrometer that sampled a 50 μm diameter circular laser spot on the sample, a power density of ~ 64 W/cm^2 caused a slow decrease in the 1108 and 1340 cm^{-1} Raman bands of NAB over a period of 10 seconds of laser exposure. The same sample observed with a line focus of 50 μm × 5 mm and a power density of 0.12 W/cm^2 exhibited negligible changes in intensity with laser exposure, and completely adequate signal-to-noise ratio spectra were obtained.

RESULTS AND DISCUSSION

Raman spectra for 4.6 nm films of NAB on both PPF and smooth Ag are shown in Fig. 1. The spectra are very similar in both peak positions and relative intensities to each other, as well as to those reported previously for a PPF substrate.[17,33] The NAB spectrum and band assignments have been analyzed in some detail,[17,33] but some bands of current relevance are the phenyl–NO$_2$ stretch (1108 cm^{-1}), the phenyl–NN stretch (1141 cm^{-1}), the NO$_2$ stretch (1340 cm^{-1}), and the N=N stretches (1401 and 1450 cm^{-1}). The observation that the NAB spectra are very similar on both PPF and Ag implies that the structure and bonding of NAB on both surfaces are similar, presumably with a phenyl–Ag bond being formed in the case of Ag. We reported previously that diazonium reagents formed either Cu–phenyl or Cu–O–phenyl bonds on copper surfaces, depending on the presence of Cu oxide initially.[34] A detailed X-ray photoelectron spectroscopy (XPS) analysis was not carried out in the present work, so there is a possibility of either Ag–C or Ag–O–C bonding between Ag and NAB. The qualitative similarity of the NAB spectra on PPF, smooth Ag, and rough Ag is reasonable for a case in which the NAB structure is similar in all three cases, and the nature of the NAB–surface bond does not significantly perturb the spectrum.

While the spectra of NAB on Ag and PPF are qualitatively similar, the PPF spectrum is significantly more intense, by a factor of approximately 5 for equal laser power, exposure time, and NAB multilayer thickness (4.5 nm). This difference is reproducible and is much larger than sample-to-sample and focusing variations. Since PPF is essentially sp^2 hybridized carbon, it would not be expected to exhibit significant electromagnetic (EM) field enhancement of Raman scattering, and smooth Ag would also not be expected to provide significant EM enhancement.[35] If some EM field enhancement results from defects on the smooth Ag, then truly smooth Ag would be expected to produce even weaker scattering than that observed in Fig. 1. We reported previously that NAB has unusually strong Raman scattering on carbon surfaces, with a surface cross-section about 10^2–10^3 times stronger than the value observed in solution.[18,19] A possible origin of this large and apparently "chemical" enhancement is revealed in Fig. 2, which compares the UV-Vis spectra of NAB in solution and chemisorbed on PPF or Ag. The apparent negative absorbance observed for NAB on Ag is presumably caused by the antireflection properties of the organic thin film, since an
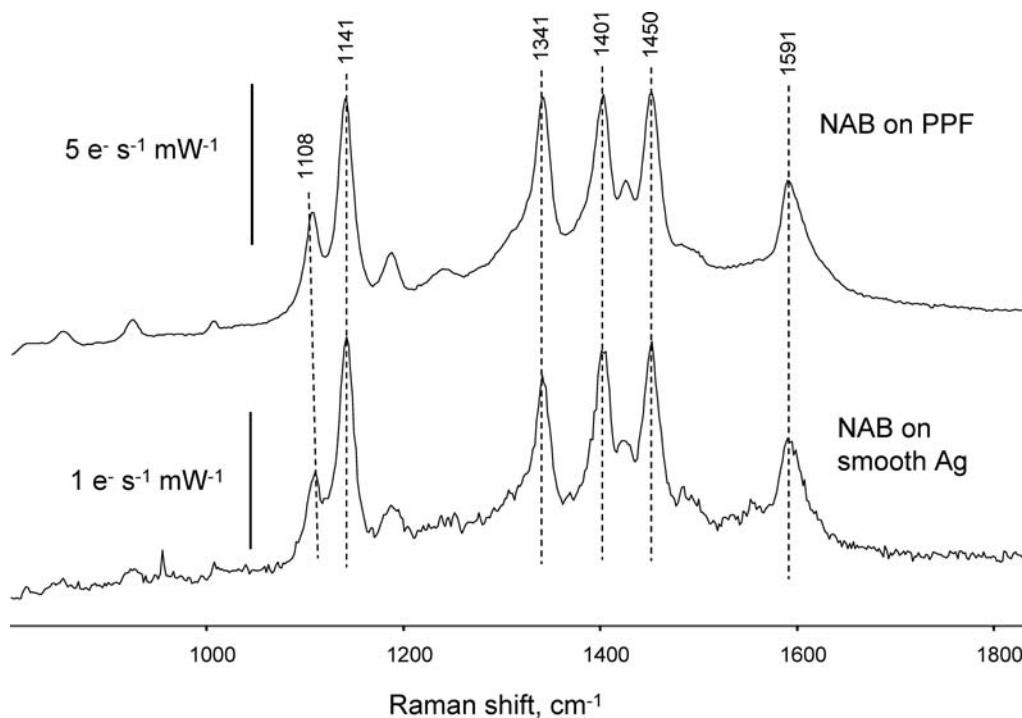
FIG. 1. Raman spectra of nitroazobenzene (NAB) films on (*top*) PPF and (*bottom*) smooth Ag. Film thickness was 4.6 nm in both cases. The scale bar indicates that the spectrum on PPF is approximately 5 times more intense than that on Ag for the same laser power and integration time. Both spectra are averages of ten 30-second CCD exposures, and a spectrum of unmodified PPF was subtracted from the NAB/PPF Raman spectrum to produce the upper spectrum.

unmodified Ag/Cr film was used as a reference. For both Ag and PPF substrates, the NAB spectrum is significantly perturbed relative to the solution spectrum, with the UV-Vis absorbance significantly shifted to longer wavelengths. The origin of the double peak in the NAB/Ag spectrum is unknown, but it is not inherent to NAB, since it was also observed with biphenyl-modified Ag. The lower wavelength peak at 318 nm matches the peak absorption for unmodified Ag/Cr on quartz and may be a subtraction artifact. For NAB on both PPF and smooth Ag, a likely source of the strong surface Raman scattering of NAB is the increase in resonance Raman cross-section caused by the shift of NAB absorption closer to the
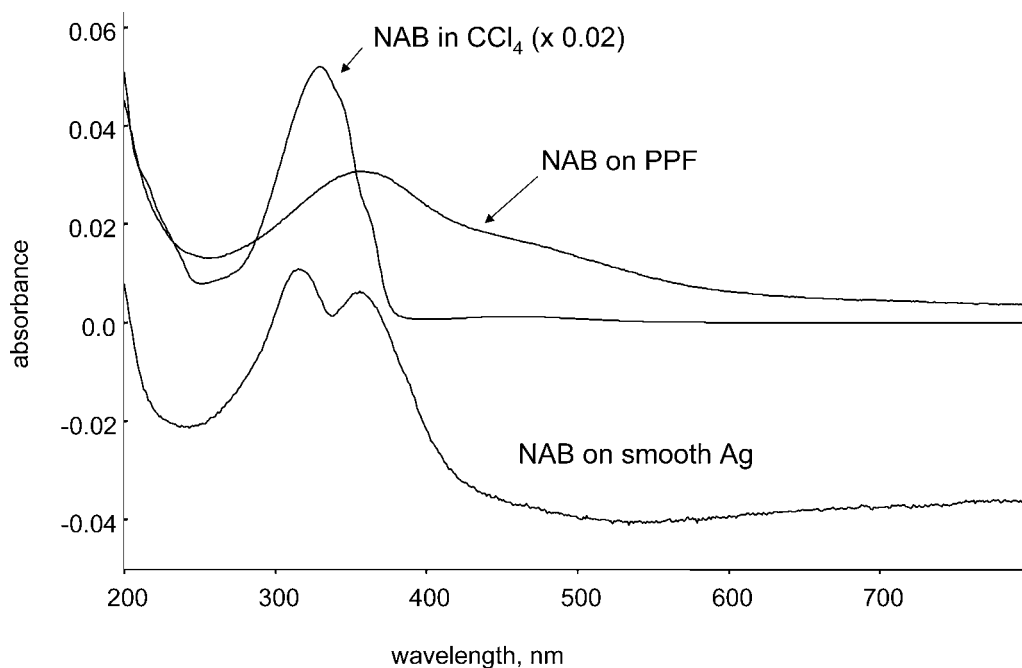

FIG. 2. UV-Vis absorption spectra of 1×10^{-5} M NAB in cyclohexane solution, NAB on PPF, and NAB on smooth Ag (1 mM NAB diazonium solution for 2 minutes). Pure cyclohexane, unmodified PPF, and unmodified Ag (20 nm thick on 4 nm of Cr) were used in the reference beams, respectively. The absorbance of the solution spectrum was divided by 50 to permit comparison. NAB multilayer thickness on Ag and PPF was 4.6 nm.
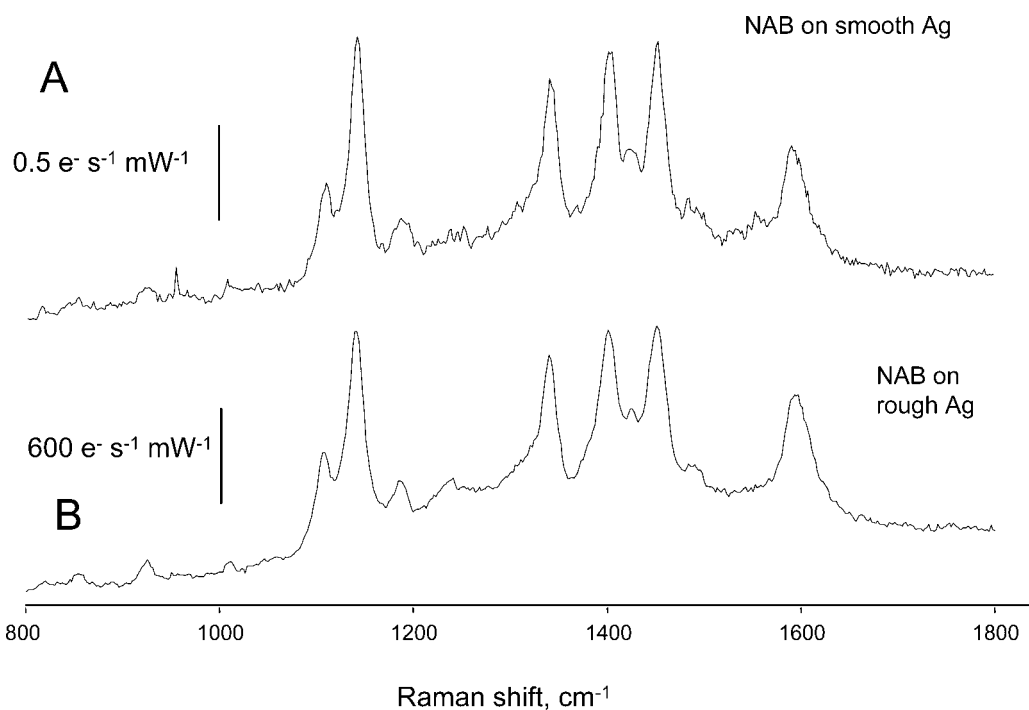
FIG. 3. Raman spectra of NAB chemisorbed to (*A*) smooth and (*B*) rough Ag. In both cases, Ag surfaces were exposed to 1 mM NAB diazonium ion in acetonitrile for 2 minutes. Note the large difference in intensity scale for the two spectra. (A) An average of five 5-second spectra with 35 mW laser power; (B) a single, 1-second exposure with 0.35 mW of laser power.

514.5 nm laser wavelength. A quantitative prediction of this resonance effect would be quite involved, but the UV-Vis and Raman spectra all imply that the electronic coupling between NAB and either PPF or Ag is strong enough to significantly perturb the surface spectra compared to free NAB in solution.

Figure 3B shows a Raman spectrum obtained on a rough Ag surface that is expected to exhibit EM field enhancement. Both smooth (Fig. 3A) and rough (Fig. 3B) Ag surfaces were exposed to 1 mM NAB diazonium ion in acetonitrile for 2 minutes, then rinsed, and observed using the line-focused Raman spectrometer. The qualitative similarity of the two spectra implies that the surface modification is similar for the two cases; however, the spectrum on rough Ag is approximately 1000 times more intense. The enhancement of surface Raman spectra by vapor deposited Ag islands is well known and results mainly from EM field enhancement.[25–29] In the case of NAB, additional enhancement results from the substantial "chemical" effect deduced from the shifts in the NAB absorption bands due to chemisorption. This "chemical" enhancement should vary significantly for different molecules depending on their absorption spectra and resonance Raman effects. In addition, it would be expected to be quite short range, and it would be smaller for multilayers than for monolayers. The SERS enhancement permits the study of much lower coverages of NAB on Ag, in principle to well below monolayer levels. Raman spectra were obtained of independent samples of rough Ag surfaces immersed for 5 seconds each in a series of NAB diazonium ion solutions ranging from 20 μM to 250 μM. The intensity of the 1591 cm^{-1} band increased monotonically with concentration from approximately 470 to approximately 1330 e$^-$ s^{-1} mW^{-1} for this series. To make changes in relative intensity more apparent, the spectra were normalized to the intensity of the 1591 cm^{-1} band and plotted in Fig. 4. Figure 4A shows the normalized and

overlaid spectra for 20, 40, 60, 120, and 250 μM, while Figs. 4B and 4C show expansions of the 1060–1180 cm^{-1} and 1300–1700 cm^{-1} regions, respectively. While all of the peak intensities increase with diazonium ion concentration, the relative intensities of the 1108, 1129, 1341, 1401, and 1442 cm^{-1} bands decrease compared to the 1591 cm^{-1} band. In addition, the relative intensities of the 1141 and 1450 cm^{-1} bands increase with concentration, and the 1396 cm^{-1} band apparent in the 20 μM spectrum shifts to 1401 cm^{-1} for the 250 μM spectrum. In order to estimate the NAB thickness on these samples, smooth Ag was subjected to the same modification conditions and examined with ellipsometry. The apparent thickness increased roughly linearly from 0.06 ± 0.06 nm to 2.10 ± 0.19 nm for the 20 to 250 μM concentration range.

Table I lists the observed band frequencies for several cases, along with values calculated with Gaussian 03 software for the model compound 4-phenyl 4'nitroazobenzene. The 20 μM peak frequencies for NAB on Ag correlate well with the "submonolayer" frequencies reported previously[33] for PPF. Furthermore, both the Ag and PPF spectra show the shift to higher frequency for the 1128, 1396, and 1443 cm^{-1} bands as the NAB coverage increases from a submonolayer (<1 nm) to a multilayer (>2 nm), as judged from ellipsometry. These spectroscopic changes are likely due to the dimerization reaction proposed by us[30,36] and others[37–41] to explain multilayer formation upon reduction of diazonium ions. Electrons transferred through the initial NAB monolayer to the diazonium ion in solution may generate another NAB radical, which attacks the monolayer, presumably at the readily accessible position ortho to the nitro group. Abstraction of the resulting H atom at the sp^3 hybridized center returns aromaticity to the first NAB molecule, and additional electrons may transfer through the dimeric layer to cause further film growth. The fact that the spectral changes apparent in Figs. 4B
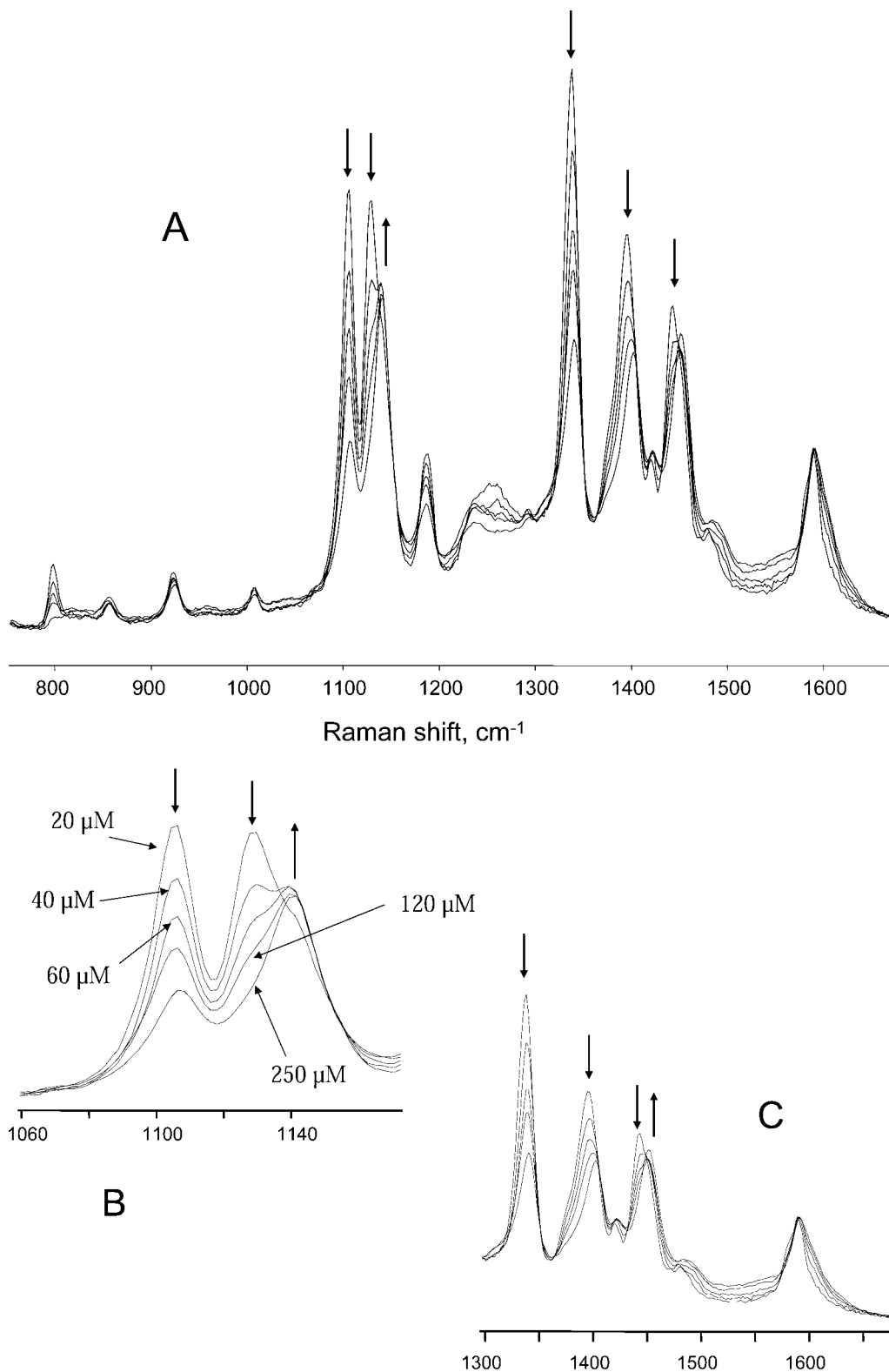
FIG. 4. Raman spectra of NAB on rough Ag surfaces for varying concentrations of NAB diazonium salt solution. Ag surfaces were exposed for 5 seconds in 20, 40, 60, 120, and 250 μM NAB diazonium tetrafluoroborate in acetonitrile, then immediately rinsed with acetonitrile and examined with Raman spectroscopy at low power density. Spectra were normalized to the 1598 cm^{-1} band intensity to permit comparisons of relative intensity. (**A**) The 800 to 1700 cm^{-1} range; (**B** and **C**) expanded spectra for selected regions. Arrows indicate the trend of various peaks with increasing concentration. All spectra were obtained with a 1-second integration time and a power density of 0.4 W/cm^2.

TABLE I. Raman band frequencies for NAB on rough Ag and PPF surfaces.

Assignment	Ag, 20 μM, 5 s	Ag, 250 μM, 5 s	Ag, 1 mM, 2 min	Submonolayer on PPF[a]	NAB on PPF[a]	Calculated for 4-phenyl NAB[a]
NO$_2$ bend	857	856	854	855	853	804
CH bend	923	924	925	924	924	934
Phenyl–NO$_2$ stretch	1107	1105	1107		1108	1086
Phenyl–NN stretch	1129	1141	1141	1124, 1137[b]	1140	1127
CH bend	1186	1187	1186	1186	1187	1172
NO$_2$ stretch	1339	1340	1340	1338	1341	1337
NN stretch + ring A[c]	1396	1401	1401	1401	1403	1394
NN stretch	1443	1451	1451	1448	1452	1454
CC ring stretch	1589	1591	~1594	1595	1595	1589
Ellipsometric thickness,[d] nm	0.06	2.1	4.4			
AFM thickness,[d] nm			4.6	0.6	4.5	

[a] From Ref. 33.
[b] Shoulder.
[c] Ring A is adjacent to the nitro group.
[d] Obtained on smooth Ag treated the same way as the rough Ag samples.

and 4C begin to occur at low concentration ($<$40 μM) implies that multilayer formation is quite facile in the case of NAB, which may be related to its relative ease of reduction. An alternative explanation for the relative intensity changes is variation of the orientation of the NAB molecule with concentration, although this effect alone cannot account for spectral changes related to multilayer formation.

The rough Ag surface is unsuitable as a substrate for molecular junctions, due to likely short circuits that would occur when a top contact is deposited on the irregular Ag/molecule surface. An alternative approach is to deposit Ag onto PPF modified with NAB in a fashion that produces a Ag pattern likely to generate significant EM field enhancement. Figure 5 shows a video micrograph of a PPF/NAB surface following vapor deposition of 10 nm of Ag through a 300 lines/inch metal grid. The value of this treatment for Raman spectroscopy is illustrated in Fig. 6 for the case of azobenzene (AB) on PPF. The lower spectrum (Fig. 6A) is that of the PPF substrate, while the spectrum in Fig. 6B shows PPF following modification by reduction of azobenzene diazonium reagent. AB is a somewhat weaker scatterer than NAB but is still significantly resonance enhanced. Subtraction of the PPF

FIG. 5. Video micrograph of PPF/AB sample following deposition of 10 nm of Ag through a 300 lines/inch copper grid.

spectrum from PPF+AB yields the spectrum of chemisorbed AB without any EM field enhancement from Ag (Fig. 6C). The spectrum shown in Fig. 6D is from the same sample following deposition of 10 nm of Ag through a 300 lines/inch metal screen, thus producing ~50 × 50 μm^2 squares of Ag in a regular array. The spectrum shown in Fig. 6D is approximately 100 times more intense than the spectrum obtained without Ag, although the two spectra are qualitatively very similar. Furthermore, the AB spectrum in Fig. 6D is much stronger than the PPF background, and it was not necessary to subtract the PPF background. Deposition of Ag squares directly on PPF led to an approximately four-fold intensity increase, much less that the factor of 100 observed for AB. Furthermore, the Ag squares are in contact with the AB but spatially separated from the PPF, thus contributing to the greater EM field enhancement for AB over PPF. It should be noted that the 50 μm squares are much larger than the ~0.1 μm Ag features that are optimal for SERS,[25–28] and it is likely that most of the EM enhancement results from the irregular edges of the Ag squares, which undoubtedly are rough on the submicrometer scale.

The SERS effect evident in Fig. 6 should be quite useful for observing molecular layers that are not resonance enhanced and therefore should broaden the utility of Raman for examining molecular junctions. The electromagnetic enhancement of SERS is not a resonance effect and should be present for most molecules close to Ag "islands". However, Ag is capable of reacting with certain monolayers, similar to results reported previously involving titanium and other metals.[33,42] Figure 7 shows the case of Ag squares deposited on an NAB layer bonded to PPF. The spectrum in Fig. 7B is very similar to that shown in Fig. 1, but with an expanded wavenumber scale. While deposition of Ag squares yields a much stronger spectrum with minimal contribution from PPF (Fig. 7 7C), the NO$_2$ stretch (1340 cm^{-1}) is weaker relative to the 1591 cm^{-1} band, and the relative intensities of the N=N stretches (1401 and 1450 cm^{-1}) have changed. As reported elsewhere, these changes are consistent with partial reduction of NAB[17,33,43] by the deposited Ag atoms.

Taken as a whole, the results permit several useful conclusions about molecular layers formed by diazonium reduction on conducting surfaces. First, bonding to both carbon and Ag surfaces is quite strong, with a covalent bond with carbon and copper well established by past evidence[19,34,41] and a covalent bond likely for Ag. Second, the surface-bound NAB
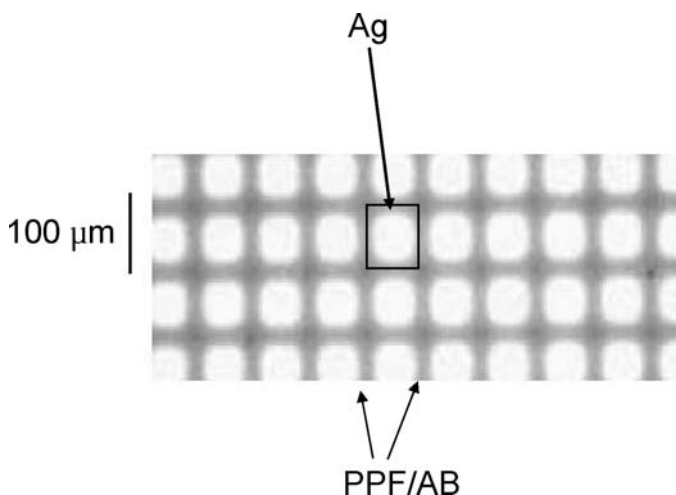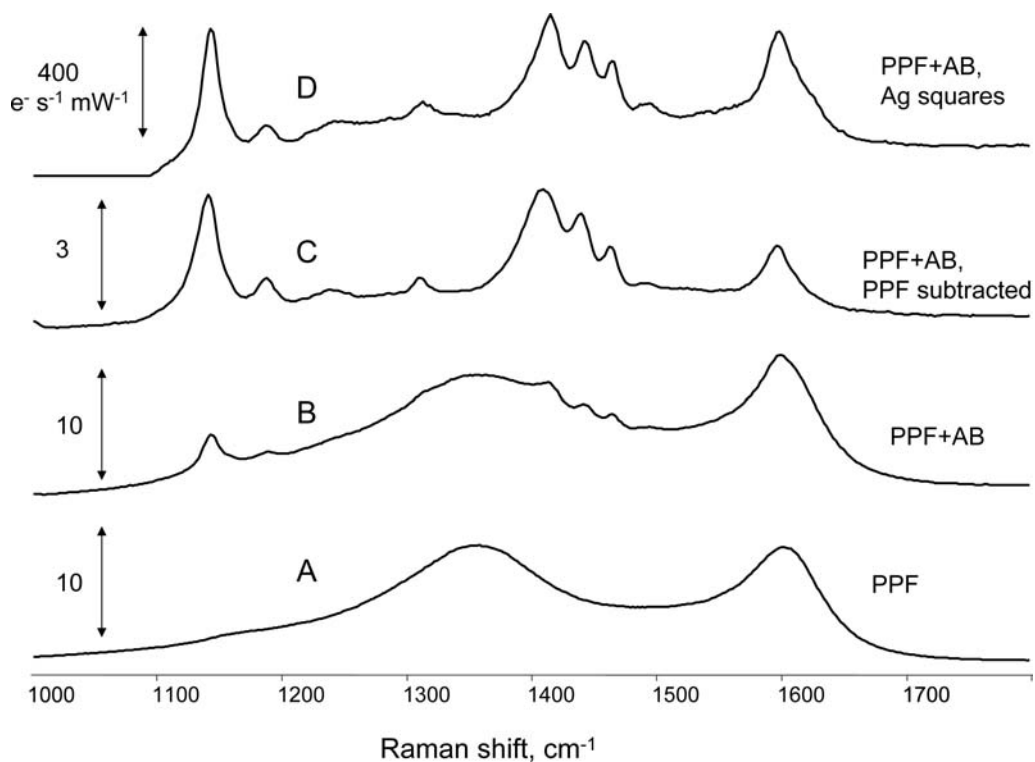
FIG. 6. Raman spectra of PPF before and after modification with azobenzene and Ag squares. (*A*) PPF substrate alone; (*B*) PPF following electrochemical reduction of azobenzene diazonium ion; (*C*) difference between spectra B and A; (*D*) PPF+AB following deposition of 10 nm of Ag through a 300 lines/inch nickel mesh. Note major change of intensity scale for spectrum D compared to A–C.
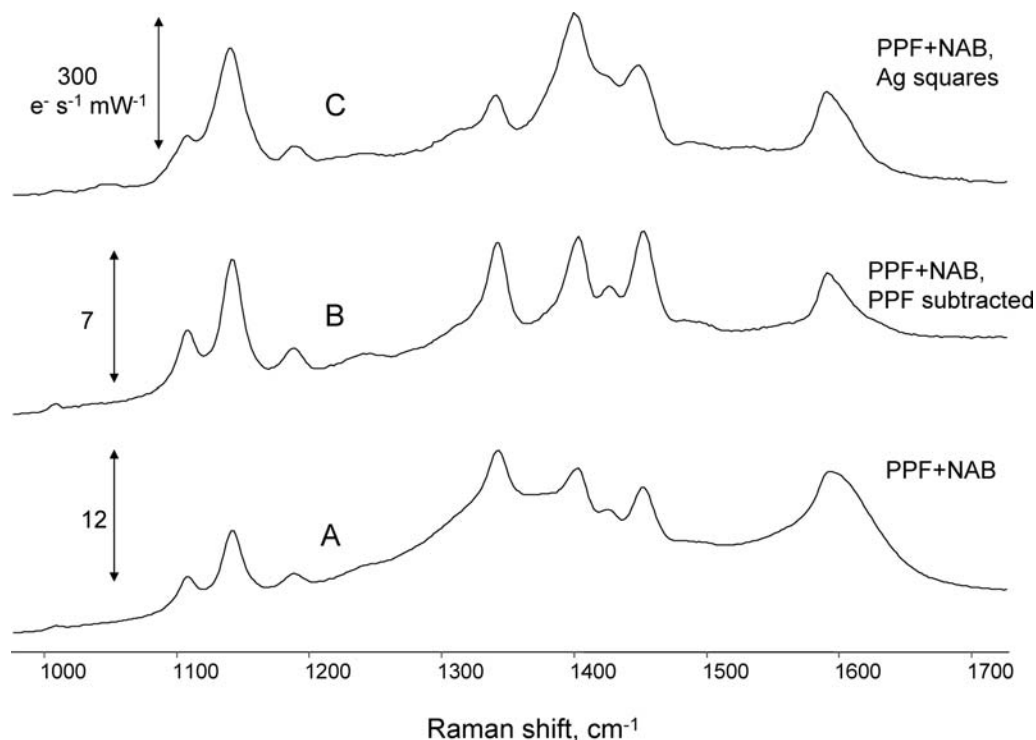

FIG. 7. Raman spectra of NAB on PPF before and after deposition of Ag squares. (*A*) and (*B*) were obtained without Ag present, with (B) being the NAB spectrum following subtraction of the PPF background. (*C*) was obtained after Ag deposition, with a very different intensity scale.

molecules exhibit a significant red shift of the UV-Vis absorption spectrum, with a larger effect observed on carbon. The shift is a good indication of significant electronic coupling between the chemisorbed NAB and the conducting substrate. In the case of an sp^2 hybridized carbon surface, this coupling may take the form of conjugation between the phenyl ring of NAB and the phenyl rings in the carbon substrate. Third, Raman scattering from NAB is strongly enhanced on both carbon and smooth Ag, with presumably negligible contribution from electromagnetic field enhancement. The enhancement is substantially greater on the carbon surface and correlates with the larger red shift of the NAB absorption spectrum. Since the red shift brings the NAB absorption closer to the 514.5 nm laser wavelength of the Raman spectrometer, the unusually strong scattering of surface bound NAB is likely to be a resonance effect. Fourth, very low concentrations of NAB diazonium ion are required to avoid multilayer formation during spontaneous chemisorption of NAB to silver. Shifts in peak positions and relative intensities correlate with multilayer formation, with the most affected bands being those associated with the azo N=N group. The most obvious indicator of multilayer formation is the shift of the phenyl–NN stretch from <1130 cm^{-1} in the submonolayer to >1140 cm^{-1}. Fifth, deposition of Ag squares on top of NAB and AB films on PPF results in enhancement of Raman scattering by a factor of approximately 100, presumably due mainly to EM field enhancement near the edges of the Ag squares. We have shown elsewhere that Ag may be used in molecular junctions as either the substrate or top contact,[20] provided the Ag is not biased too positive. We are currently examining molecular junctions of the type PPF/NAB/Ag squares/Au in order to obtain Raman spectra of molecular junctions under bias. Preliminary experiments indicate that strong SERS enhancement is maintained following deposition of a partially transparent Au layer on top of the Ag squares. Assuming the factor of 100 is maintained after depositing a metal contact on top of the Ag squares, the enhancement should permit a much wider variety of molecular junction structures to be monitored spectroscopically during operation.

ACKNOWLEDGMENT

1. M. Galperin, A. Nitzan, M. A. Ratner, and D. R. Stewart, J. Phys. Chem. B **109,** 8519 (2005).
2. A. Facchetti, M. Yoon, C. Stern, G. Hutchison, M. Ratner, and T. Marks, J. Am. Chem. Soc. **126,** 13480 (2004).
3. R. McCreery, Chem. Mater. **16,** 4477 (2004).
4. R. M. Metzger, Chem. Phys. **326,** 176 (2006).
5. Z. Zhu, T. A. Daniel, M. Maitani, O. M. Cabarcos, D. L. Allara, and N. Winograd, J. Am. Chem. Soc. **128,** 13710 (2006).
6. Y. Selzer, M. A. Cabassi, T. S. Mayer, and D. L. Allara, J. Am. Chem. Soc. **126,** 4052 (2004).
7. E. DeIonno, H.-R. Tseng, D. D. Harvey, J. Stoddart, and J. Heath, J. Phys. Chem. B **110,** 7609 (2006).
8. Y. Selzer, L. Cai, M. Cabassi, Y. Yao, J. Tour, T. Mayer, and D. Allara, Nano. Lett. **5,** 61 (2005).
9. Y. Selzer and D. Allara, Annu. Rev. Phys. Chem **57,** 593 (2006).
10. Y. Selzer, M. A. Cabassi, T. S. Mayer, and D. L. Allara, J. Am. Chem. Soc. **126,** 4052 (2004).
11. G. V. Nazin, X. H. Qiu, and W. Ho, Science (Washington, D.C.) **302,** 77 (2003).
12. K. Moth-Poulsen, L. Patrone, N. Stuhr-Hansen, J. B. Christensen, J.-P. Bourgoin, and T. Bjornholm, Nano. Lett. **5,** 783 (2005).
13. G. P. Lopinski, D. J. Moffat, D. D. M. Wayner, M. Z. Zgierski, and R. A. Wolkow, J. Am. Chem. Soc. **121,** 4532 (1999).
14. S. N. Patitsas, G. P. Lopinski, O. Hul'ko, D. J. Moffatt, and R. A. Wolkow, Surf. Sci. **457,** L425 (2000).
15. R. L. McCreery, Anal. Chem. **78,** 3490 (2006).
16. R. P. Kalakodimi, A. Nowak, and R. L. McCreery, Chem. Mater. **17,** 4939 (2005).
17. A. Nowak and R. McCreery, J. Am. Chem. Soc. **126,** 16621 (2004).
18. Y.-C. Liu and R. L. McCreery, Anal. Chem. **69,** 2091 (1997).
19. Y.-C. Liu and R. L. McCreery, J. Am. Chem. Soc. **117,** 11254 (1995).
20. S. Ssenyange, H. Yan, and R. L. McCreery, Langmuir **22,** 10689 (2006).
21. R. L. McCreery, J. Dieringer, A. O. Solak, B. Snyder, A. Nowak, W. R. McGovern, and S. DuVall, J. Am. Chem. Soc. **125,** 10748 (2003).
22. S. Ranganathan and R. L. McCreery, Anal. Chem. **73,** 893 (2001).
23. S. Donner, H. W. Li, E. S. Yeung, and M. D. Porter, Anal. Chem. **78,** 2816 (2006).
24. M. W. Williams and E. T. Arakawa, J. Appl. Phys. **43,** 3460 (1972).
25. W. B. Lacy, L. G. Olson, and J. M. Harris, Anal. Chem. **71,** 2564 (1999).
26. P. A. Schueler, J. T. Ives, F. DeLaCroix, W. B. Lacy, P. A. Becker, J. Li, K. Caldwell, B. Drake, and J. M. Harris, Anal. Chem. **65,** 3177 (1993).
27. D. J. Walls and P. W. Bohn, J. Phys. Chem. **93,** 2976 (1989).
28. S. E. Roark, D. J. Semin, and K. L. Rowlen, Anal. Chem. **68,** 473 (1996).
29. W. B. Lacy, J. M. Williams, L. A. Wenzler, T. P. Beebe, and J. M. Harris, Anal. Chem. **68,** 1003 (1996).
30. F. Anariba, S. H. DuVall, and R. L. McCreery, Anal. Chem. **75,** 3837 (2003).
31. S. Ranganathan, R. L. McCreery, S. M. Majji, and M. Madou, J. Electrochem. Soc. **147,** 277 (2000).
32. J. D. Ramsey, S. Ranganathan, J. Zhao, and R. L. McCreery, Appl. Spectrosc. **55,** 767 (2001).
33. A. M. Nowak and R. L. McCreery, Anal. Chem. **76,** 1089 (2004).
34. B. L. Hurley and R. L. McCreery, J. Electrochem. Soc. **151,** B252 (2004).
35. A. Campion, Annu. Rev. Phys. Chem. **36,** 549 (1985).
36. A. O. Solak, L. R. Eichorst, W. J. Clark, and R. L. McCreery, Anal. Chem. **75,** 296 (2003).
37. J. K. Kariuki and M. T. McDermott, Langmuir **17,** 5947 (2001).
38. J. K. Kariuki and M. T. McDermott, Langmuir **15,** 6534 (1999).
39. C. Combellas, F. Kanoufi, J. Pinson, and F. Podvorica, Langmuir **21,** 280 (2005).
40. A. Adenier, E. Cabet-Deliry, A. Chaussé, S. Griveau, F. Mercier, J. Pinson, and C. Vautrin-Ul, Chem. Mater. **17,** 491 (2005).
41. J. Pinson and F. Podvorica, Chem. Soc. Rev. **34,** 429 (2005).
42. R. McCreery, J. Wu, and R. J. Kalakodimi, Phys. Chem. Chem. Phys. **8,** 2572 (2006).
43. T. Itoh and R. L. McCreery, J. Am. Chem. Soc. **124,** 10894 (2002).